Soft Matter

PAPER

View Article Online
View Journal | View Issue

Cite this: *Soft Matter*, 2016, **12**, 7166

Static and dynamic behaviour of responsive graphene oxide–poly(*N*-isopropyl acrylamide) composite gels

B. Berke,[ab] O. Czakkel,*[a] L. Porcar,[a] E. Geissler[c] and K. László[b]

Received 18th March 2016,
Accepted 28th July 2016

DOI: 10.1039/c6sm00666c

www.rsc.org/softmatter

Thermoresponsive hydrogels have enormous potential *e.g.*, as sensors, actuators, and pollution control remedies or in drug delivery systems. Nevertheless, their application is often restricted by physical limitations (poor mechanical strength and uncontrolled thermal response). Composite systems may offer a means of overcoming these limitations. This paper presents a systematic study of the structure and dynamics of graphene oxide–poly-(*N*-isopropylacrylamide) composite systems, and investigates the effect of the nanoparticle filler content on the mechanical and swelling properties of the systems. A combination of macroscopic (swelling and elastic modulus) and microscopic (differential scanning microcalorimetry, small angle neutron scattering and neutron spin-echo spectroscopy) investigations reveals that the architecture of the polymer network is modified by chain nucleation at the surface of the GO platelets, and these form a percolating network inside the gel. Our results show that the elastic modulus of the gels is reinforced by the filler, but the mobility of the polymer chains in the swollen state is practically unaffected. The macroscopic deswelling of the composites, however, is slowed by the kinetics of ordering in the GO network.

Introduction

Responsive hydrogels are three-dimensional polymer networks with high water content.[1,2] They exhibit a reversible volume phase transition (VPT) under certain conditions.[3,4] This response can be induced by changing the environment, such as the nature of the swelling medium (composition,[5] pH[6]), temperature,[7] electromagnetic field,[8] *etc.* Among temperature sensitive responsive hydrogels those based on poly-(*N*-isopropylacrylamide) (PNIPA) are distinguished by their peculiar volume phase transition temperature (TVPT) around 34 °C, close to the temperature of the human body.[9,10] In the VPT of PNIPA, the swelling medium of the polymer, along with its dissolved ions, molecules, or drugs, is released into the surroundings. This property opens the route to various applications that require targeted delivery of drugs. The gels are relatively deformable and – owing to their high water content and the physiochemical similarity of the network to the native extracellular matrix – are potentially biocompatible.

Although their properties make them excellent candidates for applications in drug delivery,[10,11] sensors,[12] actuators,[13,14] microvalves[15] and pollution control, they have certain drawbacks. Their poor mechanical strength for example bars their use in load-bearing applications. Limited drug uptake and its non-uniform distribution within the system, particularly in the case of hydrophobic drugs, could also compromise certain applications. Furthermore, high water content combined with very wide pores often results in uncontrolled and/or undesirably rapid drug release,[16,17] which can be detrimental in targeted drug delivery systems.

These challenges may conceivably be overcome by composite hydrogels. Carbon nanoparticles are widely used as polymer fillers, with a positive impact both on the physical and the chemical properties of composites. Moreover, their density is low and they are easily recycled. Carbon black, consisting of almost pure elemental carbon, has been the most commonly used carbon filler for many years.[18] Graphite has also been used for a long time, mainly to enhance the thermal and electrical conductivity of polymers.[19] Recent developments in nanotechnology have raised interest in polymer composites containing carbon nanofibers and nanotubes. The carbon nanoparticles that have been the most intensely studied in the past few years are graphene and its derivatives.[19–22] Nanocomposites containing members of the graphene family, especially graphene oxide (GO),[23–25] have become the focus of interest. GO is considered to be non-toxic and highly biocompatible,[26] which favours its use in biomedical applications. Moreover, incorporation of GO gives visible[27] or near infrared light sensitivity to the composite systems,[28–30] which extends their potential, for example, as NIR controlled

[a] *Institut Laue Langevin, CS 20156, F – 38042 Grenoble Cedex 9, France. E-mail: czakkel@ill.eu; Tel: +33 476207182*
[b] *Department of Physical Chemistry and Materials Science, Budapest University of Technology and Economics, 1521, Budapest, Hungary*
[c] *Laboratoire Interdisciplinaire de Physique, CNRS and Université Grenoble Alpes, 38000 Grenoble, France*

microvalves, artificial muscles or actuators. Potential applications are numerous, but the detailed properties of graphene-based composites remain to be explored. In recent years several groups have reported on GO containing PNIPA gels [*e.g.* see ref. 23–25, 28 and 31–35], but direct comparison of the results is difficult, as the preparation methods differ significantly. The majority of the studies have addressed PNIPA systems of relatively high cross-link density ([monomer]/[cross-linker] $\leq$ 100), and functionalised GO nanoparticles are often used to ensure first order bond formation.[23,24] Studies using as-prepared GO as a filler have also been made.

In addition to the structural characteristics and direct information about drug release efficiency,[10,36] knowledge of the dynamics of nanocomposite systems is of crucial importance for sensing and controlled release applications. Such investigations could, however, prove difficult at the nanoscale level, owing to the limited number of appropriate methods. Dynamic light scattering (DLS) is a widely used technique for investigating dynamics in gels,[37,38] but it is inapplicable to non-transparent systems, such as those containing carbon nanoparticles. Neutron spin-echo (NSE) spectroscopy[39] can overcome these difficulties. The NSE technique is well suited for measuring slow (nanosecond timescale) dynamics in soft matter systems, with the highest energy resolution among all types of neutron spectrometers. It has proved to be an excellent tool for investigating dynamics in polymer gels.[40–45] It has been a fertile source of important new insights into polymer melt–silica nanocomposite systems,[46,47] but to our knowledge, no investigation of PNIPA hydrogel composite systems using NSE has yet been reported in the literature.

Here we present a systematic study of the structural and dynamical properties of GO containing PNIPA hydrogels in which results from macroscopic [elastic modulus measurements and differential scanning microcalorimetry (MicroDSC)] and microscopic [small angle neutron scattering (SANS) and NSE] length scales are compared.

Experimental

Graphene oxide (GO)

Graphene oxide (GO) was obtained by the improved Hummers' method[48] from natural graphite (Graphite Tyn, GK, China). The GO suspension was purified and mildly exfoliated by centrifuging 5 times (7000*g*) from 1 M HCl and 6–9 times (15 100*g*) from doubly distilled water, in order to remove unreacted graphite and inorganic salts. After the final washing and centrifugation step a light brown suspension with a GO nanoparticle content of $\sim$1 w/w% was obtained. Its C/O ratio, determined by XPS, was 2.2.

Gel synthesis

The PNIPA polymer gel was synthesised from the *N*-isopropylacrylamide (NIPA) monomer (Tokyo Chemical Industry, Japan) and the *N*,*N*′-methylenebisacrylamide (BA) cross-linker (Sigma Aldrich) in aqueous medium at 20 °C by free radical polymerization. The reaction was initiated by ammonium persulphate (APS, Sigma Aldrich) and *N*,*N*,*N*′,*N*′-tetramethylethylenediamine (TEMED, Fluka). For the synthesis of a pure PNIPA gel with a cross-linking ratio [NIPA]/[BA] = 150, 18.75 ml of a 1 M aqueous solution of NIPA and 1.225 ml of a 0.1 M solution of BA were mixed with 4.9 ml of water and 25 μl of TEMED. Finally, 1.25 ml of a 10 w/w% solution of APS was added to the mixture, and polymerization took place at 20 °C. Films of thickness 2 and 4 mm and 10 × 10 mm isometric cylinders were prepared. All chemicals were used as received, except NIPA, which was recrystallized from a toluene–hexane mixture. Doubly distilled water was used for the synthesis, purification and measurements.[38] To obtain hybrid gels with <20 mg of GO/g NIPA content the aqueous GO suspension of the required concentration was mixed with the precursor solution of the gel. The total volume of the precursor solution, including the GO suspension, was kept constant by adding the appropriate complement of water. Gels with the highest filler content (21 mg GO/g NIPA) were prepared by adding solid NIPA and BA directly to the GO suspension. The reaction medium was stirred in an ice-bath for 15 min after addition of each component. GO filled samples were polymerised and purified in the same way as the nanoparticle-free system. The nomenclature of the samples is listed in Table 1.

Macroscopic characterisation

For the swelling experiments gel disks of diameter of 7 mm were cut from a 2 mm thick film. Prior to the experiment the disks were dried in order to determine their dry mass (m_0), and then reswollen in excess doubly distilled water thermostated at 20.0 ± 0.2 °C for one week. The equilibrium swelling degree was defined as m/m_0, where m is the mass of the swollen samples.

The elastic modulus was measured on fully swollen isometric gel cylinders using an INSTRON 5543 mechanical testing instrument at ambient temperature. Samples were compressed by 10% of their initial height in steps of 0.1 mm with a relaxation time of 4 × 4 s and a force threshold of 300 N. No barrel distortion was observed.

The macroscopic thermal response of the systems was tested by placing the samples (30 mm × 40 mm, 4 mm thick, fully swollen in D_2O at 25 °C) in closed quartz containers in an incubation oven at 41 °C for 3 weeks.

Differential scanning microcalorimetry (MicroDSC)

Scanning microcalorimetry measurements were made on ground samples using a MicroDSCIII apparatus (SETARAM, France). About 10 mg of dry gel sample were placed in contact with 500 μl of Millipore water and kept at 20 °C for 2 h to allow the gels to equilibrate in the swollen state and to obtain a stable baseline.

Table 1 Sample nomenclature

Sample name	GO content (mg GO/g NIPA)
PNIPA	0
5GO@PNIPA	5.25
10GO@PNIPA	10.50
15GO@PNIPA	15.75
20GO@PNIPA	21.00

The samples were heated to 50 °C at 0.03 °C per min scanning rate. Determination of the peak position and calculation of the specific enthalpy of the volume phase transition (ΔH_{VPT}) were performed using instrument software.

Neutron spin-echo (NSE) measurements

NSE measurements[49] were made on a IN11 spectrometer at the Institut Laue-Langevin (Grenoble, France) in the IN11A high-resolution set-up. For these experiments gel films of 4 mm nominal thickness and 3 × 4 cm cross-section were used. Prior to the measurements, the gel samples were dried, and then reswollen in excess D_2O for at least 3 days at 25.0 ± 0.1 °C. Previous measurements[50] had shown that the swelling properties of the PNIPA gel are not affected by the H_2O/D_2O isotopic substitution. The swollen samples were placed in 5 mm thick sandwich-type cells with quartz windows. To exclude air and avoid deswelling, the remaining space in the sample holder was filled with D_2O. Measurements were performed at 25.0 ± 0.1 °C in the transfer vector Q-range 0.042 Å^{-1} ≤ Q ≤ 0.209 Å^{-1}, where $Q = (4\pi/\lambda)\sin(\theta/2)$, λ being the incident wavelength of the neutrons (7.83 Å) and θ the scattering angle. The Fourier-time range covered was 0.1–30 ns. The resolution functions of the instrument were determined for the different experimental conditions using the elastic scattering of graphite. The NSE method measures directly the intermediate scattering function $I(Q,\tau)$ as a function of Q and the Fourier time τ, *i.e.*, it yields directly the time dependence of the density–density autocorrelation function.[51] The resulting intermediate scattering functions were corrected for the D_2O background dynamics.

Small angle neutron scattering (SANS)

SANS measurements were performed on the D22 small angle instrument at the Institut Laue-Langevin. The gels were swollen in D_2O in order to enhance the scattering contrast between the polymer and the matrix, and to minimize the incoherent background scattering. The incident neutron wavelength was 6 Å. Two sample-detector distances (17 m and 2 m) were used to cover the Q-range 0.004–0.5 Å^{-1}. Raw SANS data were corrected for the empty cell, dark counts, sample thickness and detector efficiency. The corrected scattering data were normalized by the incident beam flux to obtain the scattered intensity in absolute units. Data reduction was done using the GRASansP v.7.04 program.

Results and discussion

Composite systems with various GO/polymer ratios were studied systematically. The influence of the nanoparticle content on the swelling ratio in pure water and on the elastic modulus of the composites is shown in Fig. 1.

Increasing the GO content drastically decreases the swelling degree and increases the elastic modulus (Fig. 1a). A similar trend is observed in pure PNIPA gels on increasing the cross-link density,[52] but the shapes of the responses are different (Fig. 1a and b). Increasing the cross-link density of the PNIPA network (*i.e.*, decreasing the molar ratio of [NIPA]/[BA]) monotonically changes the swelling degree and the elastic modulus, whereas when the GO loading is increased a plateau is observed in both quantities. Li also reported an increase in modulus when chemically modified GO is used as a co-monomer.[23] In gels with higher cross-link density (molar ratio of [NIPA]/[BA] = 35 instead of 150), addition of unmodified GO to the precursor solution results in an opposite tendency in both the swelling ratio and elastic modulus.[24,25] In the present systems the elastic modulus and the observed swelling ratio are strongly correlated (Fig. 1c). In pure PNIPA gels with different cross-link densities, the dependence of the modulus on the equilibrium polymer volume fraction ϕ ($\phi \approx 1/(\rho \times$ swelling ratio), taking $\rho = 1.115$ g cm^{-3} as the density of the dry polymer[38]) could be described by an apparent power law with an exponent of ~2.07, as expected under good solvent conditions.[52–54] In the GO@PNIPA systems the exponent is ~3.2 (Fig. 1c), which could perhaps be interpreted as a sign of the theta solvent condition.[55] This interpretation, however, is inconsistent with the rest of the observations. During the polymerisation the GO particles not only contribute to nucleating the reaction at their surfaces but also act as a filler in the network. With increasing GO content, the gel is reinforced by the filler and the architecture of the network is increasingly dominated by cross-link hypernodes, at the expense of the simple tetrafunctional cross-link structure that prevails with *N*,*N*′-methylenebisacrylamide

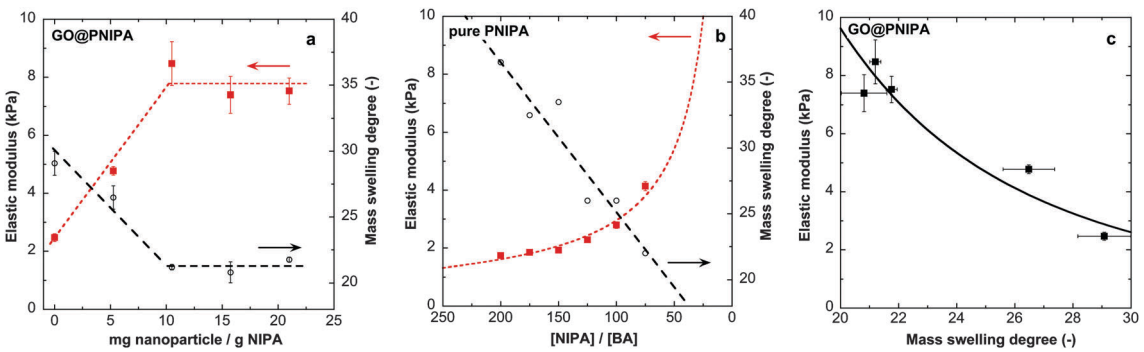

Fig. 1 Equilibrium mass swelling degree in pure water at 20 °C and the elastic modulus of (a) GO@PNIPA hybrid gels and (b) the pure PIPA gel from ref. 52. Note that a high [NIPA]/[BA] molar ratio means low cross-link density. Broken lines are guides for the eye. (c) Correlation between the elastic modulus and the observed equilibrium swelling degree in GO@PNIPA systems. Solid line is a power law fit with an exponent of 3.2.

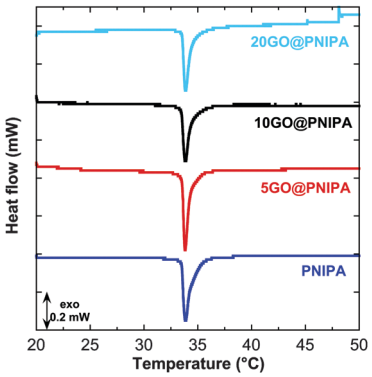

Fig. 2 Differential scanning calorimetry results of PNIPA and GO@PNIPA gels. Curves are shifted vertically for clarity.

alone. At the percolation threshold, the GO particles establish an interpenetrating network inside that of the polymer. Fig. 1a suggests that the percolation threshold of the GO occurs at a concentration of 10 mg g^{-1} dry PNIPA, *i.e.*, roughly $c_p \approx 0.5$ mg g^{-1} of the swollen gel.

The MicroDSC measurements show that T_{VPT} (33.8 °C) is unaffected by the presence of GO (Fig. 2), which implies that, while part of the polymer chains are tightly bound to the GO surface, the rest remain freely surrounded by solvent and subject to excluded volume conditions. This picture is corroborated by the fact that in the pure PNIPA gel the enthalpy of the phase transition is unaffected by changes in cross-link density,[52] whereas when the GO content is increased ΔH_{VPT} decreases monotonically (Table 2). The observed decrease in enthalpy by 18.9 J g^{-1} in the 20GO@PNIPA sample implies that 21 mg of GO reduce the number of free chains by 27%. This means that GO immobilises more than 10 times its own mass of PNIPA.

On the macroscopic scale the thermal responses of the two systems are substantially different (Fig. 3). Whereas the pure PNIPA gel reaches its fully deswollen state after less than 2 h of incubation at 41 °C, almost no size change is observed in the GO@PNIPA systems within this timescale. By contrast, at longer times the highest GO content sample responds most strongly to the temperature increase, with a final size smaller than that of pure PNIPA. This is an unexpected result, since it is known that pure PNIPA gels in their high temperature deswollen state contain a significant fraction of trapped microscopic water droplets.[56] The present finding implies that the GO, by matching the hydrophobic/hydrophilic character of PNIPA, mediates the expulsion of the trapped water. However, the timescales are different in the two cases. In the pure PNIPA gel deswelling is

Table 2 Peak position (TVPT) and specific enthalpy (ΔH_{VPT}) of the volume phase transition from DSC measurements

Sample	T_{VPT} (°C)	ΔH_{VPT} (J g^{-1} dry sample)
PNIPA	33.8	70.4
5GO@PNIPA	33.8	65.3
10GO@PNIPA	33.8	54.6
20GO@PNIPA	33.8	51.5

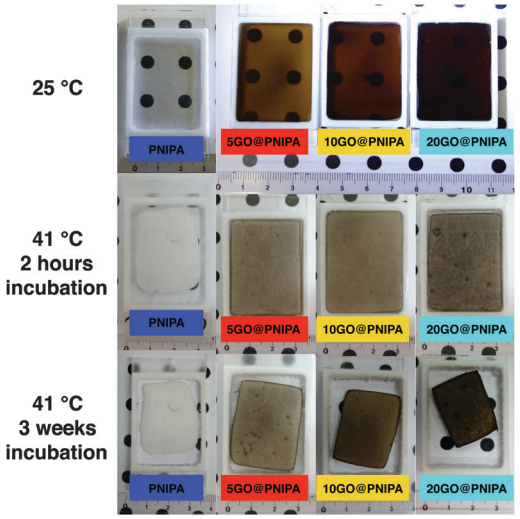

Fig. 3 Images of PNIPA and GO@PNIPA samples below (25 °C) and above (41 °C) the volume phase transition temperature at different incubation times.

governed by simple mechanical expulsion of the solvent,[57] whereas deswelling in the filled system is slowed by the kinetics of the collapse and stacking of the GO filler network. It should nevertheless be emphasized that the smaller final swelling ratio of the filled gels is the consequence not of the cross-linking by the GO but rather of the improved evacuation of water from the network. This implies that, in the collapsed state, the PNIPA chains are oriented by the GO surfaces.

To explore the structural differences caused by incorporating GO into the polymer matrix, small angle neutron scattering (SANS) measurements were performed on selected samples. In scattering experiments the detected signal depends on the contrast between the particle and the solvent. In the case of neutron scattering this contrast is defined by the difference in scattering length density (ρ) between the components. The value of ρ of the PNIPA matrix is significantly different from that of the swelling medium, namely D_2O (Table 3), resulting in a strong scattering signal. In the composite samples, which are ternary systems, the signal is still dominated by the PNIPA signal. As seen in Table 3 and Fig. 4a the neutron scattering contrast between GO and D_2O is weak, and the overall signal therefore originates almost exclusively from the polymer, even in the composite systems.

Small differences are visible in the shapes of the SANS response curves of the three investigated systems (Fig. 4a). The continuous lines through the background-subtracted data (Fig. 4b) are the modified Ornstein–Zernike (OZ) expression (eqn (1)),[55,58] which yields a good fit to all three curves in the

Table 3 Neutron scattering length densities (ρ) of the components

Component	ρ (10^{-6}/Å^2)
PNIPA $(C_6H_{11}NO)_n$	0.825
GO $C_{65}O_{35}$	5.993
D_2O	6.364

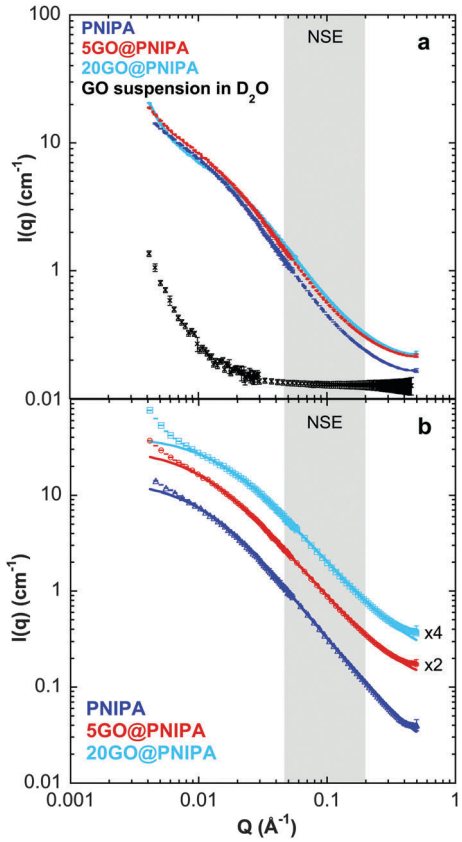

Fig. 4 (a) SANS response curves of PNIPA (dashed lines), 5GO@PNIPA (dots) and 20GO@PNIPA (continuous lines) gels swollen in D_2O, at 25 °C. Crosses are the SANS response of a GO suspension (concentration equivalent to that of the 20GO@PNIPA sample) in D_2O at 25 °C. (b) SANS response of the swollen gels (PNIPA (triangles), 5GO@PNIPA (circles) and 20GO@PNIPA (squares)) after subtraction of the corresponding backgrounds (D_2O or GO + D_2O signal). The curves are shifted vertically for clarity. Solid lines are fits to the modified Ornstein–Zernike model. Shaded areas in both figures show the Q-range of the NSE study.

range $Q > 0.01$ Å^{-1}. The deviation in the lowest Q region ($Q < 0.01$ Å^{-1}) stems from the well-known concentration inhomogeneities due to cross-linking in gel networks.[59] In the OZ model the scattered intensity can be described by

$$I(Q) = \frac{I(0)}{[I + (Q\xi)^2]^{\frac{p}{2}}} + B \qquad (1)$$

where $I(0)$ and B are Q-independent constants, ξ is the static polymer–polymer correlation length and p is the fractal dimension of the polymer coils. While ξ exhibits only a very small change at low GO content, it decreases by nearly 30% in 20GO@PNIPA (Table 4). Fig. 7 shows this variation as a function of swelling ratio (*i.e.*, inverse polymer concentration). The power law dependence is stronger than that predicted by scaling theory ($\xi \propto c^{-1.1}$ as opposed to $\xi \propto c^{-0.75}$ indicated by scaling theory[54]). In our nanocomposite systems, however, the composition of the samples is not identical, and the data therefore do not represent the same sample at different degrees of swelling.

Table 4 Characteristics of the samples from neutron scattering experiments measured at 25 °C

Sample	$D_{diff} \times 10^{11}$ (m^2 s^{-1})	ξ_H (Å)	ξ (Å)	Power law exponent
PNIPA	7.03 ± 0.14	28.4 ± 0.01	92.0 ± 1.09	1.6
5GO@PNIPA	7.41 ± 0.24	26.9 ± 0.08	90.0 ± 1.11	1.7
20GO@PNIPA	8.10 ± 0.30	24.6 ± 0.9	66.7 ± 0.67	1.6

The exponent $p = 5/3$ in eqn (1) is also consistent with the excluded volume interaction for polymer chains in good solvent.[54,55] In summary, the concentration dependence of the correlation length ξ and the excluded volume character of the exponent p imply that the network chain statistics of the gel on a length scale of $1/Q < 100$ Å are not affected by the GO.

The dynamic behaviour of the PNIPA matrix was explored by neutron spin-echo (NSE) spectroscopy. The NSE method measures the energy transfer of neutrons at extremely high energy resolution as a phase shift in the Larmor precession of the neutron spins in a magnetic field.[51] The intermediate scattering function $I(Q,\tau)$ is defined by eqn (2), as a function of Q and the Fourier time τ:

$$I(Q,\tau) = N^{-1} \sum_{k,l} \langle \exp(iQ \cdot r_k(\tau)) \exp(-iQ \cdot r_j(0)) \rangle \qquad (2)$$

where N is the number density of the system and $\langle \ldots \rangle$ means an ensemble average. The $I(Q,\tau)$ curves obtained for the pure PNIPA gel, as well as for samples 5GO@PNIPA and 20GO@PNIPA, normalized by the signal ($I(Q,0)$) of a fully elastic scatterer, are displayed in Fig. 5. As already noted, the scattering contrast between the GO and pure D_2O is small. Moreover, in the Q-range covered by the NSE measurements, the signal of the GO is matched with the solvent (see the shaded area in Fig. 4a). The observed dynamics can therefore be attributed exclusively to the motion of the chains in the polymer gel.

In all three cases the curves $I(Q,\tau)/I(Q,0)$ can be fit by a single exponential function

$$\frac{I(Q,\tau)}{I(Q,0)} \propto \exp(-\Gamma\tau). \qquad (3)$$

In the pure PNIPA gel (Fig. 5a) the curves decay to zero, indicative of practically ergodic behaviour, *i.e.*, there is no frozen-in component.[59] Fig. 1 shows that GO affects the elastic properties of the composite systems on the macroscopic scale. At the microscopic level, by contrast, the NSE results indicate that the motion of the polymer chains is only partially affected. For 20GO@PNIPA, the intermediate scattering functions (Fig. 5c) decay to a baseline value of 0.05, which corresponds to 5% immobile fraction. The GO content of this sample is about 2 w/w% of the dry content, *i.e.*, 0.1 w/w% of the swollen gel. Comparison of these findings with the microcalorimetry results of Table 1 suggests that the GO hypernodes may also partly immobilize the gel network immediately surrounding them. In the case of 5GO@PNIPA the NSE curves appear to decay to zero (Fig. 5b), as in the pure PNIPA gel. The GO content

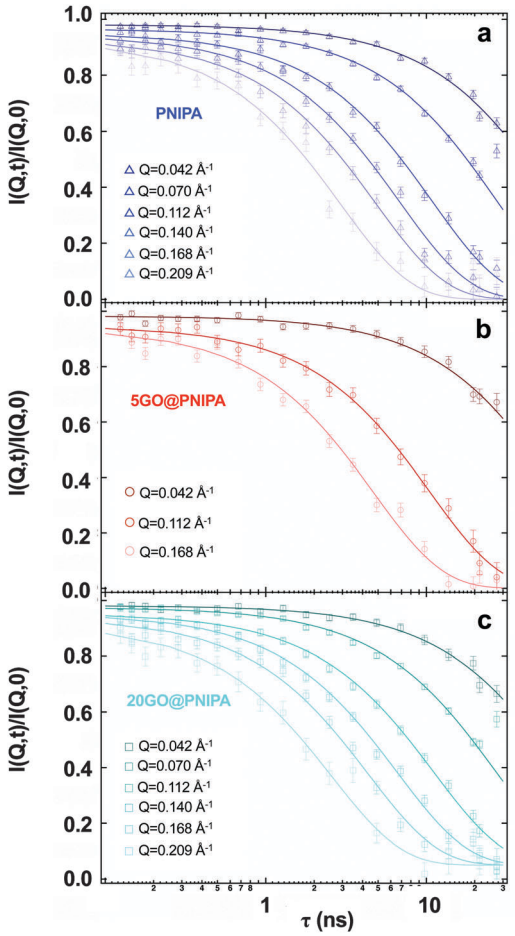

Fig. 5 Experimental intermediate scattering functions from NSE with the corresponding single exponential fits for the pure PNIPA hydrogel, 5GO@PNIPA and 20GO@PNIPA composites, measured at 25 °C.

of this gel is about 0.5 w/w%. This implies a baseline of 0.005, which is beyond the accuracy of the measurements.

The measured relaxation rates ($\Gamma = 1/\tau$) are proportional to Q^2 (Fig. 6), characteristic of diffusive motion. The diffusion coefficient (D_{diff}) is obtained directly from the linear fit

$$\Gamma = D_{\mathrm{diff}} \cdot Q^2. \quad (4)$$

With increasing GO content, owing to the lower degree of swelling, D_{diff} increases slightly (Table 4). The hydrodynamic correlation length of the samples (ξ_{H}) is determined from the Stokes–Einstein relation

$$D_{\mathrm{diff}} = \frac{k_{\mathrm{B}}T}{6\pi\eta\xi_{\mathrm{H}}} \quad (5)$$

where k_{B} is the Boltzmann constant, T is the absolute temperature, and η is the viscosity of the medium ($\eta_{D_2O,25\ ^\circ C} = 1.095 \times 10^{-3}$ N s m^{-2} [60]). Like the static correlation length, ξ_{H} decreases with increasing GO content (Table 4), albeit with a smaller exponent ($\xi_{\mathrm{H}} \propto c^{-0.43}$) than predicted by scaling theory (Fig. 7), but consistent with dynamic light scattering measurements on pure PNIPA gels.[52] This suggests that the dynamics of the polymer chains is hindered only marginally by the GO sheets.

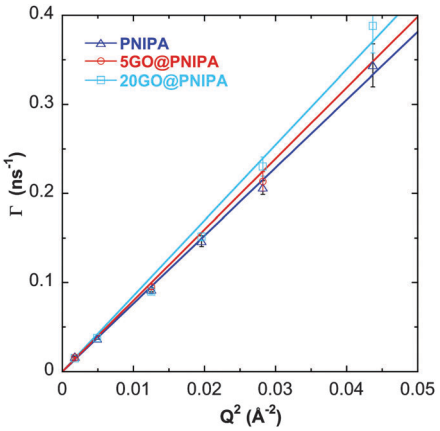

Fig. 6 Relaxation rates (Γ) *vs.* Q^2 for pure PNIPA, 5GO@PNIPA and 20GO@PNIPA. Solid lines are linear fits.

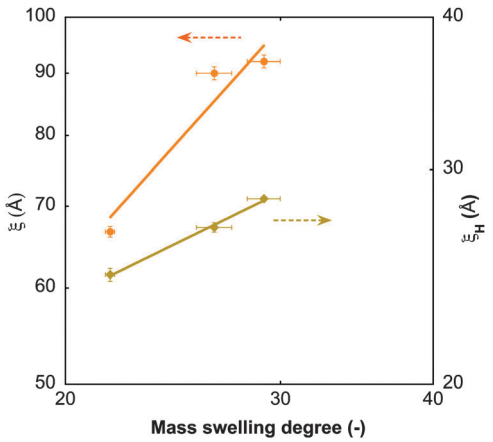

Fig. 7 Static (ξ) and hydrodynamic (ξ_{H}) correlation lengths from SANS and NSE measurements at 25 °C, as a function of the mass swelling degree of the gels. Solid lines are power-law fits to the data.

On combining these observations with macroscopic results we can conclude that GO forms a strong bonding with the PNIPA chains. As the GO concentration is low even at the highest loading, it does not affect the overall movement of

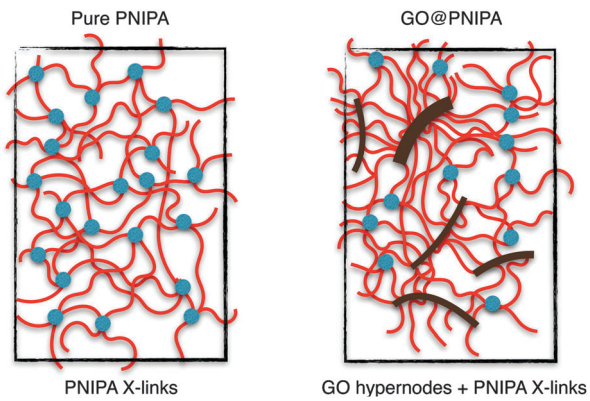

Fig. 8 Representation of the structure of pure PNIPA and GO containing PNIPA hydrogels.

the polymer chains. However, it does hinder their motion in the immediate surroundings. The reason for this may be that some of the PNIPA chains remain linked to the GO surface, even in the swollen state (Fig. 8).

Conclusions

Graphene oxide (GO) containing composite PNIPA gels were prepared and characterized both on the macro- and the nanoscale size range. Increasing the GO content reduces the swelling capacity and increases the elastic modulus of the gels. The relationship between the two properties can be described approximately by a power law with exponent ~ 3.2. This unusual behaviour is attributed to changes in the architecture of the polymer gel with the build up of an interpenetrating GO network in which the polymer matrix develops through chain nucleation at the surface of the GO. This picture is consistent with MicroDSC measurements, which show that the volume phase transition temperature of the mobile PNIPA segments is unaffected by the presence of GO, while, conversely, as the amount of bound polymer increases with increasing GO content, the enthalpy of the volume phase transition decreases. The fraction of hindered chains that are prevented from participating in the VPT amounts to more than ten times the mass of the GO filler. In the composite gels, the GO mediates the evacuation of water in the high temperature collapsed state, which, in pure PNIPA, would otherwise remain trapped in the network in the form of microscopic droplets. This implies that the collapsed PNIPA chains are oriented by the GO surfaces. The neutron scattering observations in the swollen state show that, as the gel deswells with increasing GO content, the static polymer–polymer correlation length ξ decreases according to scaling theory. The shape of the neutron scattering response is also fully consistent with scaling predictions for excluded volume interactions. The hydrodynamic properties of the network chains measured by neutron spin-echo spectroscopy are also consistent with those of the unfilled polymer gels. The correlation functions obtained from this technique also display a static component that corresponds to about 5% of the network chains in the gel that are immobilised on the GO surface. It may be speculated that the platelet structure of the GO filler modifies the hydrodynamic flow field in the vicinity of the polymer chains. Numerical comparison between the neutron spin-echo measurements and the MicroDSC measurements suggests that not all the hindered PNIPA chains are necessarily immobilized on the surface of the GO. Crowding of the chains near the surface could give rise to partial associations, which would contribute to the reduction in enthalpy at the transition.

Acknowledgements

The authors are grateful to the Institut Laue-Langevin for providing beamtime on the IN11 and D22 instruments. We thank Mr D. Renzy and Mr M. Jacques for technical assistance. The work was supported by the Hungarian grant OTKA K101861 (Hungarian Scientific Research Fund). This work is part of the scientific program "Development of quality-oriented and harmonized R+D+I strategy and functional model at BME" project supported by the New Széchenyi Plan (Project ID: TÁMOP-4.2.1/B-09/1/KMR-2010-0002).

Notes and references

1 N. K. Singh and D. S. Lee, *J. Controlled Release*, 2014, **193**, 214.
2 J. Kopecek, *Biomaterials*, 2007, **28**, 5185.
3 J. H. Bradbury, M. D. Fenn and I. Gosney, *J. Mol. Biol.*, 1965, **11**, 137.
4 M. Heskins and J. E. Guillet, *J. Macromol. Sci., Part A: Pure Appl.Chem.*, 1968, **2**, 1441.
5 T. Tanaka, *Phys. Rev. Lett.*, 1978, **40**, 820.
6 J. Ricka and T. Tanaka, *Macromolecules*, 1984, **17**, 2916.
7 Y. H. Bae, T. Okano and S. Wan Kim, *J. Polym. Sci., Part B: Polym. Phys.*, 1990, **28**, 923.
8 S. Reinicke, S. Döhler, S. Tea, M. Krekhova, R. Messing, A. M. Schmidt and H. Schmalz, *Soft Matter*, 2010, **6**, 2760.
9 K. Depa, A. Strachota, M. Šlouf and J. Hromádková, *Eur. Polym. J.*, 2012, **48**, 1997.
10 D. C. Coughlan and O. I. Corrigan, *Int. J. Pharm.*, 2006, **313**, 163.
11 A. K. Bajpai, S. K. Shukla, S. Bhanu and S. Kankane, *Prog. Polym. Sci.*, 2008, **33**, 1088.
12 A. Kumar, A. Srivastava, I. Y. Galaev and B. Mattiasson, *Prog. Polym. Sci.*, 2007, **32**, 1205.
13 L. Ionov, *Mater. Today*, 2014, **17**, 494.
14 P. Kim, L. D. Zarzar, X. He, A. Grinthal and J. Aizenberg, *Curr. Opin. Solid State Mater. Sci.*, 2011, **15**, 236.
15 S. Sugiura, K. Sumaru, K. Ohi, K. Hiroki, T. Takagi and T. Kanamori, *Sens. Actuators, A*, 2007, **140**, 176.
16 T. R. Hoare and D. S. Kohane, *Polymer*, 2008, **49**, 1993.
17 S. B. Campbell and T. Hoare, *Curr. Opin. Chem. Eng.*, 2014, **4**, 1.
18 M. Biron, *Thermosets and Composites, Material Selection, Applications, Manufacturing and Cost Analysis*, Elsevier, 2nd edn, 2013.
19 U. Szeluga, B. Kumanek and B. Trzebicka, *Composites, Part A*, 2015, **73**, 204.
20 H. Kim, A. A. Abdala and C. W. Macosko, *Macromolecules*, 2010, **43**, 6515.
21 K. K. Sadasivuni, D. Ponnamma, S. Thomas and Y. Grohens, *Prog. Polym. Sci.*, 2014, **39**, 749.
22 T. Kuilla, S. Bhadra, D. Yao, N. H. Kim, S. Bose and J. H. Lee, *Prog. Polym. Sci.*, 2010, **35**, 1350.
23 Z. Li, J. Shen, H. Ma, X. Lu, M. Shi, N. Li and M. Ye, *Soft Matter*, 2012, **8**, 3139.
24 C.-W. Lo, D. Zhu and H. Jiang, *Soft Matter*, 2011, **7**, 5604.
25 X. Ma, Y. Li, W. Wang, Q. Ji and Y. Xia, *Eur. Polym. J.*, 2013, **49**, 389.
26 G. Cirillo, S. Hampel, U. G. Spizzirri, O. I. Parisi, N. Picci and F. Iemma, *BioMed Res. Int.*, 2014, **2014**, 825017.
27 D. Kim, H. S. Leeb and J. Yoon, *RSC Adv.*, 2014, **4**, 25379.
28 K. Shi, Z. Liu, Y. Y. Wei, W. Wang, X. J. Ju, R. Xie and L. Y. Chu, *ACS Appl. Mater. Interfaces*, 2015, **7**, 27289.

29 E. Manek, B. Berke, N. Miklósi, M. Sajbán, A. Domán, T. Fukuda, O. Czakkel and K. László, *eXPRESS Polym. Lett.*, 2016, **10**, 710–720.
30 C.-H. Zhu, Y. Lu, J. Peng, J.-F. Chen and J.-H. Yu, *Adv. Funct. Mater.*, 2012, **22**, 4017.
31 Y. Wu, M. Cai, X. Pei, Y. Liang and F. Zhou, *Macromol. Rapid Commun.*, 2013, **34**, 1785–1790.
32 D. Kim, H. S. Lee and J. Yoon, *Sci. Rep.*, 2016, **6**, 20921.
33 V. Alzari, D. Nuvoli, S. Scognamillo, M. Piccinini, E. Gioffredi, G. Malucelli, S. Marceddu, M. Sechi, V. Sanna and A. Mariani, *J. Mater. Chem.*, 2011, **21**, 8727.
34 L. Breuer, M. Raue, M. Kirschbaum, T. Mang, M. J. Schöning, R. Thoelen and T. Wagner, *Phys. Status Solidi A*, 2015, **212**, 1368–1374.
35 D. Kim, H. S. Lee and J. Yoon, *RSC Adv.*, 2014, **4**, 25379.
36 J. Kost and R. Langer, *Adv. Drug Delivery Rev.*, 2012, **64**, 327.
37 E. Geissler, Dynamic Light Scattering from Polymer Gels, in *Dynamic Light Scattering*, ed. W. Brown, Clarendon Press, Oxford, 1993.
38 K. László, K. Kosik, C. Rochas and E. Geissler, *Macromolecules*, 2003, **36**, 7771.
39 F. Mezei, Neutron Spin Echo, in *Lect. Notes Phys.*, ed. F. Mezei, vol. 128, 1980.
40 Y. Hertle, M. Zeiser, P. Fouquet, M. Maccarini and T. Hellweg, *Z. Phys. Chem.*, 2014, **228**, 1053.
41 T. Kanaya, N. Takahashi, K. Nishida, H. Seto, M. Nagao and T. Takeda, *Phys. Rev. E: Stat., Nonlinear, Soft Matter Phys.*, 2005, **71**, 1.
42 M. Shibayama, K. Nishi and T. Hiroi, *Macromol. Symp.*, 2015, **348**, 9.
43 T. Hellweg, K. Kratz, S. Pouget and W. Eimer, *Colloids Surf., A*, 2002, **202**, 223.
44 S. Koizumi, M. Monkenbusch, D. Richter, D. Schwahn, B. Farago and M. Annaka, *Appl. Phys. A: Mater. Sci. Process.*, 2002, **74**, 399.
45 C. Scherzinger, O. Holderer, D. Richter and W. Richtering, *Phys. Chem. Chem. Phys.*, 2012, **14**, 2762.
46 G. J. Schneider, K. Nusser, L. Willner, P. Falus and D. Richter, *Macromolecules*, 2011, **44**, 5857–5860.
47 K. Nusser, G. J. Schneider and D. Richter, *Soft Matter*, 2011, **7**, 7988.
48 D. C. Marcano, D. V. Kosynkin, J. M. Berlin, A. Sinitskii, Z. Sun, A. Slesarev, L. B. Alemany, W. Lu and J. M. Tour, *ACS Nano*, 2010, **4**, 4806.
49 O. Czakkel, B. Berke, E. Geissler and K. László, *Study of the internal dynamics of soft gel – carbon nanoparticle composite systems*, Institut Laue-Langevin (ILL), DOI: 10.5291/ILL-DATA.9-12-374.
50 K. László, DSc dissertation, Hugarian Academy of Science, Budapest, 2005.
51 *Neutron Spin Echo Spectroscopy – Basics, Trends and Applications*, ed. F. Mezei, C. Pappas and T. Gutberlet, Springer, Heidelberg, 2003.
52 K. László, K. Kosik and E. Geissler, *Macromolecules*, 2004, **37**, 10067.
53 F. Horkay and M. Zrínyi, *Macromolecules*, 1982, **15**, 1306.
54 P. G. de Gennes, *Scaling Concepts in Polymer Physics*, Cornell University Press, Ithaca, 1979.
55 L. S. Ornstein and F. Zernike, KNAW, Proceedings, 1914, **17**(II), 793.
56 K. László, A. Guillermo, A. Fluerasu, A. Moussaïd and E. Geissler, *Langmuir*, 2010, **26**, 4415.
57 K. László, A. Fluerasu, A. Moussaïd and E. Geissler, *Soft Matter*, 2010, **6**, 4335.
58 P. Pusey and W. van Meegen, *Physica A*, 1989, **157**, 705.
59 E. Geissler, F. Horkay and A. M. Hecht, *Phys. Rev. Lett.*, 1993, **71**, 645.
60 A. Vértes, S. Nagy, Z. Kulcsár, R. G. Lovas and F. Rösch, *Handbook of Nuclear Chemistry*, Springer, Dordrecht, Heidelberg, London, New York, 2011.